

Analyzing the Multiwavelength Spectrum of BL Lacertae During the July 1997 Outburst

M. Böttcher¹

Department of Space Physics and Astronomy, Rice University, MS 108,
6100 S. Main Street, Houston, TX 77005 - 1892

S. D. Bloom^{2,3}

Laboratory for High Energy Astrophysics, NASA/Goddard Space Flight Center,
Greenbelt, MD 20771

To appear in The Astronomical Journal

ABSTRACT

The multiwavelength spectrum of BL Lacertae during its July 1997 outburst is analyzed in terms of different variations of the homogeneous leptonic jet model for the production of high-energy radiation from blazars. We find that a two-component γ -ray spectrum, consisting of a synchrotron self-Compton and an external Compton component, is required in order to yield an acceptable fit to the broadband spectrum. Our analysis indicates that in BL Lac, unlike other BL Lac objects, the broad emission line region plays an important role for the high-energy emission. Several alternative blazar jet models are briefly discussed. In the appendix, we describe the formalism in which the process of Comptonization of reprocessed accretion disk photons is treated in the previously developed blazar jet simulation code which we use.

Subject headings: Gamma Rays: observations — galaxies: active — BL Lacertae
Objects: individual (BL Lacertae)

1. Introduction

A dramatic gamma-ray outburst of BL Lacertae ($z=0.069$) during July 1997 was recently reported by Bloom *et al.* 1997. BL Lac's gamma-ray activity was coincident with bright and

¹Chandra Fellow

²NAS/NRC Resident Research Associate

³Current Address: Infrared Processing and Analysis Center, Jet Propulsion Laboratory and California Institute of Technology, MS 100-22, Pasadena, CA 91125

variable emission from optical to X-rays (Noble *et al.* 1997; Mattox *et al.* 1996); however, the light curves in each waveband are too sparsely sampled to determine accurately whether they are correlated. In addition, the gamma-ray spectrum was significantly harder than in the lower intensity state, which is commonly seen for flaring blazars (Mukherjee *et al.* 1996; Mukherjee *et al.* 1997). Multiwavelength flares coincident with gamma-ray flares have also been documented for many other objects (eg., 3C 279, Wehrle *et al.* 1998; and 1406-076, Wagner *et al.* 1995). The observations during the flare will be discussed further in Section 2.

Historically, BL Lacertae was the prototypical ‘BL Lac Object’, i.e., has quasar-like continuum properties, but does usually not show emission or absorption lines (the equivalent width is $< 5 \text{ \AA}$). Though, H α emission lines have been detected in BL Lac itself during a period of several weeks in 1995 (Vermeulen *et al.* 1995; Corbett *et al.* 1996). BL Lacertae is also a member of the blazar class of objects, i.e. a radio-loud AGN which has bright and variable broadband continuum emission as well as relatively high polarization. About 50 blazars have been detected in high energy gamma-rays by the EGRET instrument, and 14 are BL Lac objects (Mukherjee *et al.* 1997).

In this paper we will examine the multiwavelength spectral energy distribution (SED; or plot of νF_ν) of BL Lac considering several emission mechanisms as the possible source of gamma-rays: synchrotron self-Compton scattering (SSC; Ghisselini *et al.* 1985; Bloom & Marscher 1996), external inverse Compton scattering with an accretion disk as the source of soft photons (ECD; Dermer *et al.* 1992), and an external inverse Compton scattering of soft photons reprocessed in broad line region clouds (ECC; Sikora *et al.* 1994). These mechanisms and the techniques used will be discussed further in Section 3. The modeling results and their implications for the nuclear environment of BL Lac are presented and discussed in Section 4. A discussion of the application of alternative — leptonic as well as hadronic — models to the broadband spectrum on BL Lacertae follows in Section 5. We summarize in Section 6. In the appendix, we discuss our numerical treatment of Compton scattering of reprocessed accretion disk radiation, which was not included in the original version of the jet simulation code used for our modeling procedure.

2. Observations

In addition to the optical (V and R band) and EGRET gamma-ray observations of Bloom *et al.* (1997), we have included additional optical ($BVRI$; Webb *et al.* 1998), radio, X-ray, and low energy gamma-ray observations from the time of the outburst. The radio observations at 2.25 and 8.3 GHz are from the Green Bank Interferometer monitoring program (Waltman *et al.* 1996), the 4, 8 and 14 GHz measurements are from the UMRAO monitoring program (Aller *et al.* 1985). The 2-10 keV ASCA X-ray spectrum (Makino *et al.* 1997) shown in Figs. 1 – 3 (thick dashed curves) are from continuous measurements of July 18.6 – 19.62 and yielded a photon spectral index of 1.44 ± 0.01 . The ASCA spectrum agrees well with the XTE PCA spectrum of Madejski *et al.* (1997a) from the same epoch, which is not plotted in the figures. Madejski *et al.* (1999)

show that the X-ray spectrum is harder than for earlier epochs, and that it is variable on time scales of approximately one day. The OSSE observations from 0.15 – 1.0 MeV have been provided by the OSSE Team (Grove & Johnson 1997).

TeV upper limits from CAT (Fleury 1997) and HEGRA (Aharonian *et al.* 1999) from observations in 1997 August are also added (filled square and circle, respectively). Although these measurements are not quite simultaneous to the remainder of the observations, they might give a rough estimate of the actual TeV flux at the time of the July 1997 outburst because the optical flux during the TeV observations was similar to the flux observed during the EGRET flare.

A reddening correction of $A_R = 0.7$ derived from $E(B - V) = 0.3$ from Vermeulen *et al.* (1995) and the extinction law of Cardelli *et al.* (1989) were applied to the optical data presented in Bloom *et al.* (1997). Webb *et al.* (1998) have used a similar correction ($E(B - V) = 0.36$). The values of the optical flux plotted in Figs. 1–3 are averages during the week of the gamma-ray flare. The optical flux exhibited short-term variability on a timescale of several hours. The error bars shown in the figures correspond to the dispersion of the optical fluxes during the observing period.

3. Outline of the model

We modelled the broadband spectrum of BL Lac with the pair plasma jet simulation code described in detail in Böttcher *et al.* (1997, hereafter BMS). In this section, we only give a short outline of the model and the assumptions.

Our model is based on various versions of leptonic jet models for blazar emission. A blob of ultrarelativistic pair plasma is moving outward from the central accretion disc along a pre-existing cylindrical jet structure, with relativistic speed $\beta_\Gamma c$ and bulk Lorentz factor Γ . In the following, primed quantities refer to the rest frame comoving with the relativistic plasma blob. At the time of injection into the jet at height z_i above the accretion disc, the pair plasma is assumed to have an isotropic momentum distribution in the comoving frame. The distribution functions at this time are power-laws, $n'(\gamma') = n_0 \gamma'^{-s}$, with low- and high-energy cut-offs $\gamma_1 \leq \gamma' \leq \gamma_2$. The total density of electrons (and positrons) in the comoving frame is n'_e . The blob is spherical in the comoving frame with radius R'_B which does not change along the jet. A randomly oriented magnetic field of strength $B' \lesssim B'_{ep}$ is present, where B'_{ep} is the magnetic field corresponding to equipartition with the energy density of pairs at the base of the jet. The jet is inclined at an angle θ_{obs} with respect to the line of sight. The spherical geometry in the comoving rest frame implies that, in the stationary frame of the AGN, the blob appears Lorentz contracted with a length parallel to the jet axis of $R_{\parallel} = R'_B/\Gamma$ and a perpendicular extent $R_{\perp} = R'_B$.

As the blob moves out, various radiation and cooling mechanisms are at work: synchrotron radiation, synchrotron self-Compton radiation (SSC; Ghisselini *et al.* 1985, Marscher & Gear 1985, Maraschi *et al.* 1992, Bloom & Marscher 1996), inverse-Compton scattering of external radiation from the accretion disc, either entering the jet directly (ECD for External Compton scattering of

direct Disc radiation; Dermer *et al.* 1992, Dermer & Schlickeiser 1993) or after being rescattered by surrounding (BLR) material (ECC for External Compton scattering of radiation from Clouds; Sikora *et al.* 1994, Blandford & Levinson 1995, Dermer *et al.* 1997). The latter process was not included in the original version of the BMS simulation code. Therefore, its treatment is described in more detail in the appendix.

The BLR is represented by a spherical layer of material with uniform density and total Thomson depth $\tau_{T,BLR}$, extending between the radii $r_{in,BLR} \leq r \leq r_{out,BLR}$ from the central black hole. The synchrotron mirror mechanism (Ghisellini & Madau 1996, Bednarek 1998) is unlikely to be efficient in BL Lac objects (Böttcher & Dermer 1998), because it requires a high Thomson depth of the surrounding material ($\tau_{T,BLR} \gtrsim 0.1$), for which no evidence exists in this class of objects. Therefore we do not consider it in our spectral modeling procedure for BL Lac.

The central accretion disc is radiating a standard Shakura-Sunyaev (1973) disc spectrum around a black hole of $10^6 M_6$ solar masses. The total disc luminosity is $10^{44} L_{44}$ erg s⁻¹. The full angle dependence of the disc radiation field, according to its radial temperature structure, is taken into account. Compton scattering of all radiation fields is calculated using the full Klein-Nishina cross section. The SSC mechanism is calculated to arbitrarily high scattering order.

After the initial injection of ultrarelativistic pairs, all of the mechanisms mentioned above (except the synchrotron mirror) are taken into account in order to follow the evolution of the electron/positron distribution functions and the time-dependent broadband emission as the blob moves out along the jet. $\gamma\gamma$ absorption intrinsic to the source and the re-injection of pairs due to $\gamma\gamma$ pair production is taken into account completely self-consistently using the exact, analytic solution of Böttcher & Schlickeiser (1997) for the pair injection spectrum due to $\gamma\gamma$ absorption. However, with the parameters adopted to fit the spectrum of BL Lac, the blob is optically thin to $\gamma\gamma$ absorption for photons up to at least 100 GeV so that this process plays a minor role. Consequently, since we assume that the blob does not expand, the total electron (positron) density n'_e in the blob remains basically constant along the jet.

The broadband spectrum investigated in this paper is a time average over the entire duration of the γ -ray flare. Thus, it corresponds to the time average of the radiation emitted by one or multiple plasma blobs rather than to a snapshot during the evolution of a single blob. To compare our model spectra to the observed broadband spectrum of BL Lacertae, we use the time-integrated broadband emission (fluence) of a single blob. An average flux is calculated by dividing the fluence by a representative time scale which corresponds to the time scale of repeated blob ejection events. A jet quasi-continuously filled with relativistic pair plasma corresponds to a repetition time of $t_{rep} = 2R'_B/(\Gamma c)$. We define a filling factor f of the jet given by $f = t_{rep}^{cont}/t_{rep}$. In all our model fits we find that the repetition time scale (in the comoving frame) is generally longer than the cooling time scale for the highest-energy electrons, but comparable to the decay time scale of radiation produced by the inefficiently cooled part of the electron spectrum. Therefore, the variability in the high-energy portions of both the synchrotron and the inverse-Compton components (optical

— UV and > 100 MeV γ -rays, respectively) is dominated by light-travel time effects within the source. These effects have recently been studied in detail by Chiaberge & Ghisellini (1998). Strong variability on the light-travel time scale through the blob is expected in the high-energy parts of both radiation components, if the filling factor is substantially less than 1. The variability in these two energy bands (optical/UV and high-energy γ -rays) is expected to be correlated. If $f \sim 1$, any variability pattern is determined by variations of the electron injection parameters (i. e. the electron density, cutoff energies, spectral index etc.) and its modelling would require additional model assumptions about the underlying accretion flow and the pair injection mechanism. The low-frequency portions of both components (radio — infrared and X-rays, respectively), which are predominantly produced by basically uncooled electrons, are expected to show relatively weak variability on longer time scales, also determined by long-term variations of the pair injection parameters.

We point out that the evolution of individual blobs is virtually independent of the existence of multiple blobs along the jet if there are no significant fluctuations of the bulk Lorentz factor Γ within the flow. The radiation emitted by each individual blob is quasi-isotropic in the comoving frame so that the radiative interaction between different blobs may be neglected. The situation investigated here is geometrically very similar to shocks propagating along the jet because for large values of Γ the blobs are strongly Lorentz contracted along the jet axis. A major difference between a shock-in-jet model and our impulsive-acceleration model is that in the case of shocks particle acceleration will continue to take place at large distances from the central engine, where the external radiation field due to direct or reprocessed accretion disk radiation is negligible. Therefore, those models will be strongly SSC dominated. The spectral signatures will be basically indistinguishable from the SSC dominated cases of our model calculations, which we will discuss in the following section.

Throughout this paper, we assume $H_0 = 65$ km s $^{-1}$ Mpc $^{-1}$ and $q_0 = 0.5$.

4. Modeling results and discussion

Apart from the observed broadband spectrum, there are several other observational results on BL Lac, which constrain the choice of parameters to be adopted in our modeling efforts. Recently, Denn et al. (1999) have observed superluminal motion in BL Lac of single components with up to $\beta_{\perp,app.} = (5.0 \pm 0.2) h^{-1} = 7.7 \pm 0.3$. This indicates that the typical bulk Lorentz factor is expected to be in the range $\Gamma \gtrsim 8$. This is much higher than the limit implied by the required transparency of the emitting region for high-energy γ -ray photons due to $\gamma\gamma$ absorption within the source, which yields

$$D \gtrsim \left(\frac{L_\gamma \sigma_T (1+z)}{4\pi m_e c^4 \Delta t_{var}} \right)^{1/5} \approx 1.4 \quad (1)$$

for a variability time scale of 1 day. Here $D = (\Gamma [1 - \beta_\Gamma \cos \theta_{obs}])^{-1}$ is the Doppler factor.

Occasionally, BL Lac shows strong emission lines. On May 21 and June 1, 1995, their width has been measured to be $\langle v \rangle \approx 4000 \text{ km s}^{-1}$ (Vermeulen *et al.* 1995, Corbett *et al.* 1996). If we attribute this width to Keplerian motion, we find for the average distance of the BLR clouds from the central black hole:

$$\bar{r}_{BLR} = 2.77 \cdot 10^{-4} M_6 \text{ pc.} \quad (2)$$

We have used the XSTAR code (Kallman & Krolik 1998) in order to estimate the emission line luminosity resulting from a BLR consisting of Thomson thick ($\tau_T \sim 10$) individual clouds, illuminated by disk blackbody radiation from an accretion disc around a black hole of $M_6 \approx 2$, radiating at a luminosity of $L_D \sim 10^{44} \text{ erg s}^{-1}$. We find that an angle-average Thomson depth $\tau_{T,BLR} \sim 0.02$ is sufficient to produce the observed line luminosity $L_{H\alpha} \sim 10^{41} \text{ erg s}^{-1}$. However, this value of the required $\tau_{T,BLR}$ is strongly dependent on the clumpiness of the BLR and may well deviate by more than an order of magnitude from the value given above.

The total luminosity of the accretion disc is poorly constrained since the spectral coverage is insufficient to clearly exclude the existence of a big blue bump from the accretion disc. We adopt a disc luminosity of $L_D = 10^{44} \text{ erg s}^{-1}$, implying that no big blue bump should be observable above the synchrotron spectrum.

The shortest observed variability timescale during the 1997 flare was several hours, observed at optical wavelengths. The variability timescale at γ -ray energies was ~ 1 day, while it was slightly shorter than a day in X-rays. The optical variability yields a constraint on the extent of the emission region of

$$R'_B \lesssim 5.4 \cdot 10^{14} D \Delta t_5 \text{ cm} \quad (3)$$

where Δt_5 is the variability timescale in units of 5 hours.

We have first attempted to fit the broadband spectrum of BL Lac with the basic models, where one of the radiation mechanisms mentioned above dominates the entire X-ray and γ -ray spectrum.

Madejski *et al.* (1999) have presented an analytical estimate of the required parameters for an SSC fit to BL Lacertae, indicating that, if the entire γ -ray spectrum, peaking at $\epsilon_{SSC} \gtrsim 2 \cdot 10^4$, where $\epsilon = h\nu/(m_e c^2)$ is the dimensionless photon energy, were produced by the SSC mechanism, unrealistic values of $\Gamma \gtrsim 100$ and $B' \lesssim 10^{-4} \text{ G}$ would be needed. As mentioned in the previous section, the same arguments would apply to an SSC dominated shock-in-jet model.

Fig. 1 illustrates our attempts to fit a strongly SSC-dominated model to the broadband spectrum of BL Lac. The optical flux and the hard X-ray and soft γ -ray spectrum are well reproduced by this model. It is also very well consistent with the concave spectral shape at

soft X-rays for which Madejski et al. (1999) have found weak evidence in ASCA observations of BL Lacertae in 1995 November, suggesting that the high-energy tail of the synchrotron component and the low-energy tail of the inverse-Compton component overlap in the 2 – 10 keV energy band. However, a pure SSC model is not able to reproduce the hard power-law above 100 MeV (EGRET). This is primarily because an SSC spectrum does not produce a strong spectral break in the MeV range which would be necessary to connect the X-ray / soft γ -ray spectrum to the EGRET spectrum. Our model γ -ray spectrum peaks at a values of ϵ_{ssc} significantly lower than $2 \cdot 10^4$, which is the only way to allow for more realistic values of Γ and B' than estimated above.

In contrast to the SSC model, a pure external inverse-Compton model does produce the necessary spectral break in the MeV energy range and therefore reproduces the OSSE – EGRET γ -ray spectrum of BL lac better (see Fig. 2). However, the spectrum predicted by the ECD-dominated model is inconsistent with the ASCA X-ray spectrum. The jet filling factor corresponding to the simulation shown in Fig. 2 is $f \approx 1$, which implies that any variability would be related to variations of the particle injection/acceleration mechanism. In order to have the ECD component strongly dominate the SSC component we need to assume a much larger mass of the central black hole ($M_6 = 100$) than for our best fit presented in Fig. 3, where $M_6 = 2$.

The parameters required for an synchrotron + ECD model to reproduce the observed luminosities and peak frequencies in the broadband spectrum of BL Lacertae can be estimated using

$$\frac{L_{ECD}}{L_{sy}} \approx \frac{u'_{ECD}}{u'_B} \approx \frac{2 L_D}{B'^2 z_i^2 c \Gamma^2}, \quad (4)$$

where z_i is the injection height of the plasma blob above the accretion disk, which is approximated by a point source located at the center of the AGN. Using

$$B' \approx B_{cr} \frac{\epsilon_D \epsilon_{sy}}{\Gamma \epsilon_{ECD}} \sim 0.9 \Gamma^{-1} \text{ G}, \quad (5)$$

where $B_{cr} = 4.414 \cdot 10^{13}$ G, we find that eq. 4 becomes independent of Γ , and

$$z_i \sim \frac{\sqrt{2}}{\sqrt{c} B_{cr}} \sqrt{\frac{L_D L_{sy}}{L_{ECD}}} \frac{\epsilon_{ECD}}{\epsilon_D \epsilon_{sy}} \sim 1.6 \cdot 10^{-2} \text{ pc}, \quad (6)$$

where $\epsilon_D \sim 10^{-4}$ is the dimensionless peak energy of the accretion disk spectrum.

Since in the ECC process the accretion disc photon energies are boosted to much higher energies into the blob rest frame, because most of the soft photons enter the blob from the front, it is not possible to produce the OSSE – EGRET spectrum of BL Lac with a single ECC radiation component. However, it is appropriate to produce the observed γ radiation in the EGRET energy range and, in particular, the spectral peak at $\epsilon_{ECC} \gtrsim 2 \cdot 10^4$ with reasonable parameters. Approximating the external photon energy density due to reprocessed accretion disk photons as

$$u'_{ECC} \approx \frac{L_D \tau_{T,BLR} \Gamma^2}{4\pi \bar{r}_{BLR}^2 c}, \quad (7)$$

we find

$$\frac{L_{ECC}}{L_{sy}} \approx \frac{2 L_D \tau_{T,BLR}}{\bar{r}_{BLR}^2 c B_{cr}^2} \left(\frac{\epsilon_{ECC}}{\epsilon_{sy} \epsilon_D} \right)^2 \quad (8)$$

or

$$\frac{\bar{r}_{BLR}^2}{\tau_{T,BLR}} \sim 2.3 \cdot 10^{33} \text{ cm}^2, \quad (9)$$

in reasonable agreement with our estimates on \bar{r}_{BLR} and $\tau_{T,BLR}$ as given at the beginning of this section, considering the uncertainty of those estimates due to the unknown degree of clumpiness of the BLR. The co-moving magnetic field may be estimated as

$$B' \sim B_{cr} \frac{\epsilon_{sy}}{\epsilon_{ECC}} \epsilon_D \Gamma \sim 0.8 \Gamma \text{ G.} \quad (10)$$

The problems with fitting a one-component X-ray / γ -ray spectrum to the SED of BL Lac lead us to the conclusion that a second component is necessary to explain its peculiar high-energy spectrum. This is in agreement with the general tendency among different subclasses of blazars found by Ghisellini et al. (1998) that the sequence HBL \rightarrow LBL \rightarrow FSRQ may be related to an increasing dominance of external Compton scattering over synchrotron self-Compton scattering in the γ -ray regime. Since the properties of BL Lacertae are found to be intermediate between classical BL Lac objects and quasars, such a combination of SSC and ERC mechanisms appears to be a natural explanation for its peculiar high-energy spectrum. For the case of BL Lacertae this conclusion was first pointed out on the basis of analytical estimates by Madejski et al. (1997b, 1999). Since the SSC mechanism yields a reasonable fit to the optical to soft γ -ray spectrum, we started out from this model and adjusted the parameters in a way that a second component shows up in the EGRET energy range. The fact that there is clear evidence for the existence of BLR clouds rather close to the central black hole, and the analytical estimates regarding this process suggest that the ECC mechanism is responsible for this additional high-energy component.

Fig. 3 shows our best fit to the SED of BL Lac. The broadband spectrum from optical to high-energy γ -rays is reasonably well reproduced by our model. However, as all of our model calculations, it underpredicts the radio flux, because the low-energy cutoff in the electron energy distribution leads to a sharp cutoff in the synchrotron spectrum below $\sim 10^{13}$ Hz. Since there is no clear evidence for a correlation between radio and γ -ray flares in blazars (Mücke et al. 1997), it seems plausible that most of the radio flux is produced in the outer jet regions, where the bulk kinetic energy of the jet is dissipated in interactions with external material. This is supported by the results of long-term radio, IR, optical, and X-ray monitoring of BL Lacertae as reported by Bregman et al. (1990). They have found that radio flux variations typically lack fluctuations at optical and IR frequencies by ~ 1 - 4 years. Their result that radio and IR flux variations are correlated with X-ray variations, but not with fluctuations of the optical flux, is consistent with

the IR and the X-ray flux being produced by strongly cooled electrons in the jet via synchrotron and SSC radiation, respectively. The radio, IR, and X-ray portions of the photon spectrum reflect long-term variations of the physical conditions at the acceleration site. Short-term variations of the injected electron spectrum are smoothed out by the slow cooling process. In contrast, the optical flux, produced by electrons cooling on much shorter time scales, reflects variations of the physical conditions on time scales comparable to the synchrotron cooling time scale of ultrarelativistic electrons. Using similar arguments, McHardy et al. (1999) have recently interpreted simultaneous IR and X-ray fluctuations of 3C 273 as evidence for the SSC process being responsible for the X-ray emission of that object.

The fact that in Figs. 1 and 3 the total spectrum (solid line) is below the (unabsorbed) SSC spectrum (long dashed), indicates that here $\gamma\gamma$ absorption becomes important. As outlined above, $\gamma\gamma$ pair production is included in our simulations self-consistently.

The blob repetition time required by our fit implies a filling factor of $f = 0.8$, which means that the jet is filled essentially continuously. As explained in the previous section, this implies that due to light-travel time effects within the blob no strong variability on time scales shorter than the light-travel time through the blob are expected (Chiaberge & Ghisellini 1998), although the cooling timescale of ultrarelativistic electrons in the blob rest frame is only a few 100 s. Source variability is directly related to variations of the injection/acceleration mechanism.

Due to the very time-consuming nature of our simulations, we cannot perform a detailed variational analysis of all parameters and give relative errors on their values. However, we point out that the relative strength of the different radiation components as well as their location in energy space constrain most of the parameters listed in the figure captions rather tightly. For example, an increase in the black hole mass leads to a) the BLR moving outward (Eq. [1]) and thus to a decrease of the ECC component, and b) the Schwarzschild radius and therefore the disc moving outward and becoming cooler, implying that the ECD component becomes stronger (because photons enter the blob under a more favorable angle), but emerges at different energies (combined effect of different disc temperature and different beaming pattern of disc radiation into the blob). Due to the colder disk, the ECC component will emerge at lower energies. Such changes also imply a change in the cooling time scale as compared to the required repetition time scale, determined by the total luminosity of a single blob which has consequences on the predicted variability pattern as mentioned in the previous section. This may indicate that the self-consistent system we simulate is rather sensitive to changes of the parameters, although there might still be ambiguities.

Our results are sensitive to the assumed injection height z_i of the blob. According to the physical picture that the blob is produced by an explosive event in a hot corona above the accretion disk, we have generally chosen $z_i \approx R_B$, since there is no obvious mechanism how relativistic particles could be transported to significant distances above the disk without radiative losses.

We find the appropriate average Thomson depth of the BLR, $\tau_{T,BLR} = 0.025$, to be

comparable to what we expect in other BL Lac objects (using the estimates given in Wandel 1997). However, since the BLR seems to be located unusually close to the accretion disc ($\bar{r} = 5.5 \cdot 10^{-4}$ pc $\approx 3 \cdot 10^3 R_S$), it can still produce a significant flux in H α line emission and contribute a significant soft photon density from rescattered accretion disc radiation. As pointed out in Böttcher & Dermer (1998), a BLR of such low Thomson depth, located so close to the central black hole is extremely inefficient in terms of the synchrotron mirror mechanism, which provides additional justification for our neglect of this process.

According to the results of Stecker & de Jager (1997), $\gamma\gamma$ absorption by the intergalactic infrared background radiation is negligible for these photon energies at the redshift of BL Lac ($z = 0.069$), so the cutoff has to be intrinsic to the source. However, the CAT and HEGRA measurements have been performed in August 1997 and were therefore not simultaneous to the rest of the broadband spectrum. Since generally blazars show the strongest and most rapid variability at the highest photon energies, the > 300 GeV flux during the EGRET outburst could well have been higher than indicated by the upper limits in Figs. 1 – 3.

Our model has generally problems with the hard optical spectrum. Although the correct optical flux is predicted, rapid cooling leads to a steep optical synchrotron spectrum $F_\nu \propto \nu^{-p/2}$ for a cooling particle population injected with a power-law $n(\gamma) \propto \gamma^{-p}$. The same problem has been encountered in other blazars, such as PKS 0528+134 (Mukherjee *et al.* 1999) where, in some observing periods, the optical spectrum indicates an upturn compared to the overall synchrotron spectrum. This upturn is clearly inconsistent with the onset of the inverse-Compton component as well as with a “big blue bump” due to direct accretion disk radiation, which, in the case of PKS 0528+134, would imply an accretion disk luminosity of $\sim 10^{48}$ erg s $^{-1}$. Up to now there is no generally accepted solution to this problem, and in most modeling efforts on the objects, it is simply ignored. A possible solution might be the effect of reacceleration, e. g. by hydromagnetic turbulences due to interactions of the jet material with the surrounding medium. Fermi acceleration by hydromagnetic turbulences will only affect the lowest-energy particles of the pair ensemble simulated here because for higher particle energies radiative losses strongly dominate reacceleration. Since the optical regime is close to the low-frequency turnover of the synchrotron component, reacceleration will thus have its dominant effect in this spectral range.

5. Discussion of alternative models

Until now, we have focused on the homogeneous, leptonic jet model characterized by instantaneous injection events of relativistic plasma blobs into the jet. We are now discussing a variety of alternative models which have also met with considerable success in explaining broadband spectra of blazars. For models invoking continuous injection of electrons into the jet, such as the accelerating-jet model discussed by Georganopoulos & Marscher (1998), the final conclusions would be very similar to those found in the analysis of our model since our fits require jet filling factors close to unity.

5.1. Shock-in-jet models

In the previous section we had already briefly mentioned that a shock propagating through the jet (e. g., Marscher & Gear 1985, Kirk *et al.* 1998) would be strongly SSC dominated, and the broadband spectrum predicted by this model would be very similar to our SSC dominated case (see Fig. 1). However, the spectrum could look drastically different if an external radiation component becomes efficient at large distances from the central engine. This external radiation component could most plausibly be provided by a cloud, reflecting part of the synchrotron radiation produced within the jet (the synchrotron mirror, Ghisellini & Madau 1996, Böttcher & Dermer 1998). Böttcher & Dermer (1998) have shown that the energy density of the reflected synchrotron radiation in the comoving frame of the disturbance may be approximated as

$$\frac{u'_{Rsy}}{u'_{sy}} \approx 4 \Gamma^3 \tau_{T,c} \frac{R'_B}{\Delta r_c} \left(1 - \frac{2\Gamma R'_B}{z}\right), \quad (11)$$

where Δr_c and $\tau_{T,c}$ are the radial extent and the Thomson depth of the reflecting cloud of cold material, and z is the distance of the disturbance from the central engine. In this model, R'_B may be identified with the extent of the disturbance along the jet (denoted x in Marscher & Gear 1985). Approximating further $u'_{sy} \approx \tau_{T,d} \langle \gamma \rangle^2 u'_B$, where $\tau_{T,d}$ is the Thomson depth of the disturbance along the jet axis, and $\langle \gamma \rangle^2 \Gamma^2 \approx \epsilon_{Rsy}/\epsilon_{sy}$, we find

$$\frac{L_{Rsy}}{L_{sy}} \approx 4 \tau_{T,d} \tau_{T,c} \Gamma \frac{R'_B}{\Delta r_c} \frac{\epsilon_{Rsy}}{\epsilon_{sy}} \left(1 - \frac{2\Gamma R'_B}{z}\right). \quad (12)$$

Eq. 12 indicates that the synchrotron mirror becomes efficient, if $z \gg \Gamma R'_B$. In the following, we will require this condition to be fulfilled. The variability time scale of a high-energy γ -ray flare in this scenario is given by $\Delta t_{var} = \max \{\Delta r_c/(\Gamma^2 c), R'_B/(\Gamma c)\}$, which yields a constraint on Δr_c in addition to the constraint on R'_B as given in Eq. 3. Using these constraints, we find

$$\tau_{T,d} \tau_{T,c} \gtrsim \frac{1}{4} \frac{L_{Rsy}}{L_{sy}} \frac{\epsilon_{sy}}{\epsilon_{Rsy}} \sim 8 \cdot 10^{-12}, \quad (13)$$

which appears to be a reasonable number. Assuming that the hard X-ray / soft γ -ray spectrum of BL Lacertae is dominated by the SSC process — as we expect in the shock-in-jet model —, and that the SSC component peaks at $2 \lesssim \epsilon_{SSC} \lesssim 200$, we derive a bulk Lorentz factor of $10 \lesssim \Gamma \lesssim 100$. Then, the condition $z \gg c\Gamma^2 \Delta t_{var}$ yields $z \gtrsim 1$ pc. Since the disturbance is emitting synchrotron and SSC radiation basically independent of the external (reflected) radiation field, we would expect an extended high state of

$$\Delta t_{sy,SSC} \sim \frac{z}{\Gamma^2 c} \gg \Delta t_{var,EGRET} \quad (14)$$

at mm, infrared, optical, UV, X-rays, and soft γ -rays prior to the EGRET flare. This seems to contradict the observed quasi-simultaneous flaring at optical frequencies and in the EGRET

energy range as reported by Bloom et al. (1997), unless the synchrotron mirror operates at very low efficiency due to $z \sim 2\Gamma R'_B$.

5.2. Leptonic cascade models

Blandford & Levinson (1995) have proposed a model invoking a pair cascade developing along the jet as synchrotron and inverse-Compton radiation produced by the accretion disk and within the jet is rescattered into the jet by circumnuclear material and initiates a pair cascade via $\gamma\gamma$ pair production with the inverse-Compton emission produced by relativistic electrons injected into the jet at the injection radius. In its original form, this model predicts single power-law high-energy spectra, but it is well conceivable that the soft and hard γ -ray spectra are composed of different radiation components, as in our model. One problem with this pair cascade model is that it predicts that the high-energy emission in the EGRET regime lags variations at lower frequencies, and the high-energy variability should be characterized by longer variability time scales, which is in contradiction to most γ -ray flares observed from blazars so far. This is because the γ -ray photosphere, beyond which the jet becomes optically thin to $\gamma\gamma$ pair production for photons of a given γ -ray energy, increases with increasing photon energy. Also, the observed quasi-simultaneity of the optical and γ -ray flares of BL Lac with probably roughly equal time scales might be hard to reproduce with this model.

A different model, also based on a leptonic pair cascade, has been suggested by Marcowith et al. (1995). In this model, the jet consists of a mildly relativistic, cylindrical outer electron-proton jet which powers an ultrarelativistic, inner pair jet via hydromagnetic interaction at the boundary between these two regions. A pair cascade is initiated by $\gamma\gamma$ absorption of inverse-Compton scattered direct accretion disk photons with themselves and the radiation field of the accretion disk. The model predicts a strong spectral break ($\alpha_\gamma \approx 2\alpha_X$) at the photon energy where $\gamma\gamma$ absorption becomes important. As in the Blandford & Levinson (1995) model, this scenario predicts a γ -ray photosphere increasing with γ -ray energy. The Marcowith et al. (1995) model has been very successful in explaining the high-energy spectrum of 3C 273, where many other models have problems with the large spectral break around ~ 10 MeV. However, in its published form, the model does not provide detailed predictions about the synchrotron component, and it predicts a smooth single power-law at high energies, inconsistent with the MeV – GeV spectrum of BL Lacertae. An additional soft photon source for inverse-Compton scattering could possibly solve the latter problem, but these issues would need to be addressed in detail by the authors of this model, before a final conclusion about its applicability to BL Lacertae can be drawn.

5.3. Hadronic models

In this subsection, we discuss models in which most of the relativistic particle energy in the jet is primarily contained in protons. Their energy can either be transferred to secondary pairs through $p\gamma$ initiated pair cascades or via collisionless acceleration mechanisms to primary electrons.

Mannheim et al. (1996) have presented a model fit of the proton-initiated cascade (PIC) model of Mannheim (1993) to a non-simultaneous broadband spectrum of BL Lacertae. This model seems to have the potential to provide a reasonable fit also to our simultaneous broadband spectrum. The hardening of the γ -ray spectrum at several GeV may be interpreted as the blue-shifted bump resulting from the decay of first-generation π^0 mesons produced in $p\gamma$ interactions. Flares at γ -ray energies are expected to be simultaneous to synchrotron flares, in agreement with the observations of BL Lacertae. For model parameters derived in the context of this model see Mannheim et al. (1996).

The second class of initially proton-dominated jet models is based on plasmoid deceleration and collisionless transfer of internal energy of swept-up protons to non-thermal electrons (Pohl & Schlickeiser 1999). The radiation signatures of these processes have been investigated in detail by Dermer & Chiang (1998) and Chiang & Dermer (1999), and their application to blazars has been discussed in Dermer (1999) and Pohl & Schlickeiser (1999). For moderate ($\Gamma \sim 10$) bulk Lorentz factors of the plasmoid SSC is so far assumed to be the primary γ -ray production mechanism. The simultaneity between the synchrotron and the γ -ray flare observed in BL Lacertae suggests that the radiative cooling time scale of non-thermal electrons in the blast wave is shorter than the dynamical time scale of the system, i. e. the electrons are in the fast-cooling regime. In this case, and if SSC scattering occurs in the Thomson regime, the γ -ray luminosity may be approximated as

$$\frac{L_{SSC}}{L_{sy}} \approx \frac{1}{3} \left(\frac{p-2}{p-1} \right) \frac{\epsilon_e}{\epsilon_B}, \quad (15)$$

where p is the spectral index of the nonthermal distribution into which electrons are accelerated, and ϵ_e and ϵ_B are the energies in nonthermal electrons and in the magnetic field as a fraction of their respective equipartition values. For a standard value of $p \sim 2.5$, this yields $\epsilon_e \sim 30 \epsilon_B$, which implies that the magnetic field strength has to be substantially below the equipartition value. This has also been found for γ -ray bursts by Chiang & Dermer (1999), where too strong a magnetic field would lead to too rapid electron cooling, producing too soft X-ray spectra, inconsistent with the hard low-energy slopes observed by BATSE. A pure SSC spectrum, however, would not produce the peculiar spectral shape of the high-energy spectrum observed in BL Lac. A solution to this problem could be a blue-shifted π^0 bump (Pohl & Schlickeiser 1999) or an additional contribution from Comptonization of an external radiation field.

6. Summary and conclusions

We have analyzed the multiwavelength data for BL Lacertae during its July 1997 outburst in terms of several popular models for the broadband emission of blazars. We found that a reasonable fit is only possible with a combined SSC/ECC model. The parameters of the central accretion disc and its environment which yield an acceptable fit are $M_{BH} = 2 \cdot 10^6 M_{\odot}$, $L_D = 10^{44} \text{ erg s}^{-1}$, $\tau_{T, BLR} = 0.025$. The minimum variability time scale consistent with our model is $\Delta t_{var, min} \sim 1.2 \text{ h}$.

The need for an external inverse-Compton component in the GeV photon energy range, in addition to the SSC component, confirms that BL Lac is an atypical BL Lac object. For example, the simultaneous broadband spectra of the X-ray selected BL Lac objects like Mrk 421 (Mastichiadis & Kirk 1997) and Mrk 501 (Pian *et al.* 1998, Petry *et al.* 1999) can very well be fitted with a pure SSC model, while the emergence of an external inverse-Compton component seems to be more typical of quasars, where strong line emission indicates the existence of relatively dense broad-line regions. In fact, most simultaneous broadband spectra of quasars during outbursts can well be fit with an ECC or ECD model (e. g., 3C273: Dermer *et al.* 1997), or a combined SSC/ECD/ECC model (e. g., PKS 0528+134: Böttcher & Collmar 1998, Mukherjee *et al.* 1999; 3C279: Hartman *et al.* 1999). This trend has been more firmly established by a detailed modeling analysis of 51 γ -ray loud blazars by Ghisellini *et al.* (1998).

Since BL Lac belongs to the subclass of radio selected BL Lac objects whose properties are generally intermediate between quasars and X-ray selected BL Lacs, our results might strengthen the hypothesis that it is the density and structure of matter surrounding the central engine of an AGN which determines its appearance as either quasar or BL Lac object. In particular, this implies that the differences between these classes of objects are not predominantly due to viewing angle effects.

Our conclusions are certainly biased in the sense that we have concentrated on leptonic jet models of impulsive particle injection, which is the only type of models which we have supported by detailed numerical simulations. We have done so because of the considerable success with which this model has met in explaining a wide variety of blazar spectra in many different γ -ray intensity states. We have discussed several alternative models, such as shock-in-jet models, leptonic cascade models and hadronic jet models. Several of these possibilities could not be ruled out. Detailed numerical calculations of the application of those models to our simultaneous broadband spectrum of BL Lacertae are beyond the scope of this paper, but we strongly encourage the authors of those models to do similar analyses so that a definitive conclusion in favor of a single model can be reached.

This research has made use of data from the University of Michigan Astronomy Observatory, which is supported by the National Science Foundation and by funds from the University of Michigan. We also note that the Green Bank Interferometer is a facility of the National Science

Foundation operated by the National Radio Astronomy Observatory in support of the NASA High Energy Astrophysics programs.

SDB has conducted this research as a National Research Council Resident Associate. The work of MB is supported by NASA through Chandra Postdoctoral Fellowship grant PF 9-10007 awarded by the Chandra X-ray Center, which is operated by the Smithsonian Astrophysical Observatory for NASA under contract NAS 8-39073.

We thank the referee for inspiring comments and suggestions, and J. Mattox, A. Marscher and P. Sreekumar for many useful discussions.

A. Reprocessed accretion disc radiation

For the effects of Compton scattering of accretion-disc radiation rescattered into the jet trajectory by surrounding clouds, the central accretion disc may be treated as a point source, radiating isotropically, since in the process of rescattering in the BLR, virtually all spatial information about the point of origin of photons in the accretion disc gets lost. Furthermore, the accretion disc spectrum is approximated by a single-temperature blackbody spectrum. The blackbody temperature $\Theta_D = kT_d/(m_e c^2)$ is determined in a way that the resulting spectrum peaks at the same photon energy as the total photon spectrum of the Shakura-Sunyaev (1973) disc. This yields the photon production rate of the disc,

$$\dot{N}_D^*(\epsilon_D^*, \Omega_D^*) = \frac{K}{4\pi} \frac{\epsilon_D^*{}^2}{e^{\epsilon_D^*/\Theta_D} - 1} \quad (\text{A1})$$

where K is determined by the normalization to the total disc luminosity L_D ,

$$K = \frac{L_D}{m_e c^2} \frac{15}{\Theta_D^4 \pi^4} \text{ sr}^{-1} = 1.88 \cdot 10^{49} \frac{L_{44}}{\Theta_D^4} \text{ s}^{-1} \text{ sr}^{-1}. \quad (\text{A2})$$

Throughout the appendix, the asterisk denotes quantities in the accretion disc rest frame, whereas quantities without asterisk denote quantities in the blob rest frame. $\epsilon = h\nu/(m_e c^2)$ is the dimensionless photon energy, and $\Omega_D^* = (\mu_D^*, \phi_D^*)$ is the solid angle of emission of an accretion disc photon with respect to the jet axis.

Following the treatment of rescattering in surrounding material as outlined in Böttcher & Dermer (1995), but for a time-independent situation, we find for the differential photon number of rescattered accretion disc photons at height z above the disc, in the stationary frame,

$$n_{ph}^*(\epsilon^*, \Omega^*; z) = \frac{\sigma_T K}{16 \pi^2 c} \frac{\epsilon^*{}^2}{e^{\epsilon^*/\Theta_D} - 1} \int_{r_{min}}^{r_{max}} dr \frac{n_e(\mathbf{r}) x}{r |z^2 - x^2 - rz \mu_D^*|}, \quad (\text{A3})$$

where r is the distance of the scattering location in the BLR from the center of the accretion disc (the black hole), and $x = \sqrt{r^2 + z^2 - 2rz\mu_D^*}$. μ_D^* follows from simple geometrical considerations, $n_e(\mathbf{r})$ is the electron density in the BLR at the location \mathbf{r} which is determined by r and μ_D^* . This photon density is transformed to the blob rest frame using the Lorentz invariance of $n_{ph}(\epsilon, \Omega)/\epsilon^2 = n_{ph}^*(\epsilon^*, \Omega^*)/\epsilon^{*2}$ and

$$\epsilon^* = \epsilon \Gamma (1 + \beta_\Gamma \mu), \quad (\text{A4})$$

$$\mu^* = \frac{\mu + \beta_\Gamma}{1 + \beta_\Gamma \mu}, \quad (\text{A5})$$

where μ and μ^* are the angle cosine under which the photon enters the blob in the comoving and the stationary frame, respectively. The photon spectrum (A3) is used in the procedure described in BMS to calculate the electron energy-loss rate and the emitted photon spectrum due to inverse-Compton scattering.

If the blob is located well within the inner boundary of the BLR, $z \ll r_{in, BLR}$, the energy-loss rate can be well approximated assuming that all rescattered photons enter the blob from the front, i. e. with $\mu = -1$. This is the head-on approximation. Furthermore, in this case we approximate the photon spectrum by a delta-function in photon energy,

$$\frac{\epsilon^3}{e^{\frac{\epsilon}{\Theta_D} \Gamma(1 + \beta_\Gamma \mu)} - 1} \longrightarrow B_2 \delta(\epsilon - \langle \epsilon \rangle) \quad (\text{A6})$$

where

$$\langle \epsilon \rangle \approx 2.7 \frac{\Theta_D}{\Gamma(1 + \beta_\Gamma \mu)} \quad (\text{A7})$$

and

$$B_2 = \frac{\pi^4}{15} \left(\frac{\Theta_D}{\Gamma(1 + \beta_\Gamma \mu)} \right)^4. \quad (\text{A8})$$

Combining these two approximations yields

$$\begin{aligned} - \left(\frac{d\gamma}{dt} \right)_{ECC}^{\delta, \text{head-on}} &= \gamma^2 \frac{\pi^2}{960} \sigma_T^2 K \Theta_D^4 \Gamma^2 (3 + \beta_\Gamma^2) \cdot \\ I(\langle \epsilon \rangle, \gamma, -1) &\int_{r_{min}}^{r_{max}} dr \frac{x n_e(\mathbf{r})}{r |z^2 - x^2 - rz\mu_D^*|}, \end{aligned} \quad (\text{A9})$$

where $\langle \epsilon \rangle = 2.7 \Gamma \Theta_D$. The integral I involves the angle integrations over the Klein-Nishina cross section, to which an analytical solution is given in BMS. In our simulations, this approximation is used as long as $z < 0.2 \cdot r_{in, BLR}$. In this range, its deviation from the exact electron energy-loss rate is negligible for all electron energies.

If

$$\gamma_2 \ll \frac{1}{2.7 \Gamma \Theta_D}, \quad (\text{A10})$$

the entire scattered photon spectrum may be calculated in the Thomson regime. In this case, it is given in the blob rest frame by

$$\dot{n}_{ECC}^{Th}(\epsilon_s, \Omega_s) = \frac{\sigma_T^2 K}{32 \pi^2} \int_{-1}^1 d\mu \int_1^\infty d\gamma \frac{n(\gamma)}{\gamma^2} \frac{\epsilon^2}{e^{\epsilon \frac{\Gamma(1+\beta\Gamma\mu)}{\Theta_D}} - 1} \int_{r_{min}}^\infty dr \frac{n_e(\mathbf{r}) x}{r |z^2 - x^2 - r z \mu_D^*|} \quad (\text{A11})$$

where $\epsilon = \epsilon_s / (\gamma^2 [1 - \beta \chi])$ and $\chi = \mu \mu_s$ is the cosine of the collision angle between the scattering electron and the photon before scattering. Here, we have neglected the very weak dependence of the scattered photon spectrum on the azimuthal angles involved. In our simulations, we use Eq. (A11) if $\gamma_2 \leq 0.1 / (2.7 \Gamma \Theta_D)$.

REFERENCES

Aharonian, F., et al., 1999, A&A, in press (astro-ph/9903455)

Aller, H. D. *et al.* 1985, ApJS, 59, 513

Bednarek, W., 1998, A&A, 336, 123

Blandford, R. D., & Levinson, A., 1995, ApJ, 441, 79

Bloom, S. D. & Marscher, A. P. 1996, ApJ, 461, 657

Bloom, S. D., et al., ApJ, 490, 145

Böttcher, M., & Collmar, W., 1998, A&A, 329, L57

Böttcher, M., & Dermer, C. D., 1995, A&A, 302, 37

Böttcher, M., & Dermer, C. D., 1998, ApJL, 501, L51

Böttcher, M., Mause, H., & Schlickeiser, R., 1997, A&A 324, 395 (BMS)

Bregman, J. N., et al., 1990, ApJ, 352, 574

Cardelli, J. A., Clayton, G. C., & Mathis, J. S., 1989, ApJ, 345, 245

Chiaberge, M., & Ghisellini, G., 1998, MNRAS, 306, 551

Chiang, J., & Dermer, C. D., 1999, ApJ, 512, 699

Corbett, E. A. et al. 1996, MNRAS, 281, 737

Denn, G. R., Mutel, R. T., & Marscher, A. P., 1999, ApJ, submitted

Dermer, C. D., Schlickeiser, R., & Mastichiadis, A., 1992, A&A, 256, L27

Dermer, C. D., 1999, Astrop. Phys., 11, 1

Dermer, C. D., & Chiang, J., New Astronomy, 3, 157

Dermer, C. D. & Schlickeiser, R., 1993, ApJ, 416, 458

Dermer, C. D., Sturner, S. J., & Schlickeiser, R. 1997, ApJS, 109, 103

Fleury 1997, private communication

Georganopoulos, G., & Marscher, A. P., 1998, ApJ, 506, 621

Ghisellini, G., Maraschi, L., & Treves, A., 1985, A&A, 146, 204

Ghisellini, G. & Madau 1996, MNRAS, 280, 67

Ghisellini, G., Celotti, A., Fossati, G., et al., 1998, MNRAS, 301, 451

Grove, J. E. & Johnson, W. N., 1997, IAU Circular 6705

Hartman, R. C., et al., 1999, in preparation

Kallman, T. R., & Krolik, J. H., 1998, The XSTAR Manual

Kirk, J. G., Rieger, F. M., & Mastichiadis, A., 1998, A&A, 333, 452

Madejski, G., et al., 1997, IAU Circular 6705

Madejski, G., et al., 1997, AAS High Energy Astrophysics Division Meeting, Estes Park, Colorado

Madejski, G., et al., 1999, ApJ, 521, 145

Makino, F., et al. 1997, IAU Circular 6708

Mannheim, K., 1993, A&A, 269, 67

Mannheim, K., Westerhoff, S., Meyer, H., & Fink, H. H., 1996, A&A, 315, 77

Maraschi, L., Ghisellini, G., & Celotti, A., 1992, ApJ, 397, L5

Marcowith, A., Henri, G., & Pelletier, G., 1995, MNRAS, 277, 681

Marscher, A. P. & Gear, W. K., 1985, ApJ, 298, 114

Mastichiadis, A., & Kirk, J. G., 1997, A&A, 320, 19

Mattox, J. R. et al. 1996, ApJ, 461, 396

McHardy, I., Lawson, A., Newsam, A., Marscher, A. P., Robson, I., & Stevens, J., 1999, MNRAS, in press (astro-ph/9907383)

Mücke, A., et al., A&A, 320, 33

Mukherjee, R. et al. 1996, ApJ, 470, 831

Mukherjee, R. et al. 1997, ApJ, 490, 116

Mukherjee, R., et al., 1999, ApJ, 527, in press (astro-ph/9901106)

Noble, J. C. et al. 1997, IAU Circular 6693

Petry, D., et al., 1999, ApJ, submitted

Pian, E., et al., 1998, ApJ, 429, L17

Pohl, M., & Schlickeiser, R., 1999, A&A, submitted

Shakura, N. I., & Syunyaev, R. A., 1973, A&A, 24, 337

Sikora, M., Begelman, M. and Rees, M. 1994, ApJ, 421, 153

Stecker, F. W., & de Jager, O. C., 1997, ApJ, 476, 712

Vermeulen et al. 1995, ApJ, 452, 5

Wagner, S. et al. 1995, ApJ, 454, L97

Waltman, E. et al 1996, AJ, 112, 2690

Wandel, A., 1997, ApJ 490, L131

Webb, J. R. et al 1998, AJ, 115, 2244

Wehrle, A., et al., 1998, ApJ, 497, 178

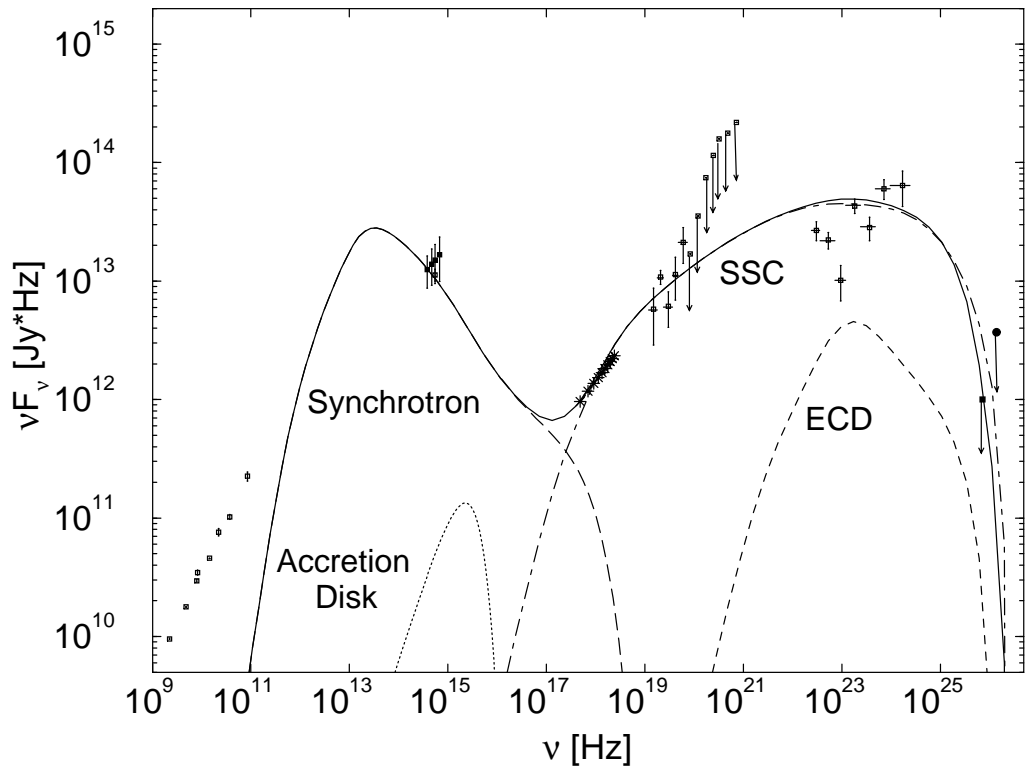


Fig. 1.— Attempt to fit the SED of BL Lac with an SSC-dominated model. Parameters: $\gamma_1 = 3000$, $\gamma_2 = 10^5$, $s = 2.6$, $B' = 1.2$ G, $\Gamma = 15$, $\theta_{obs} = 2^\circ$, $n'_e = 10^3$ cm $^{-3}$, $R'_B = 10^{15}$ cm, $z_i = 10^{-3}$ pc, $f = 0.6$

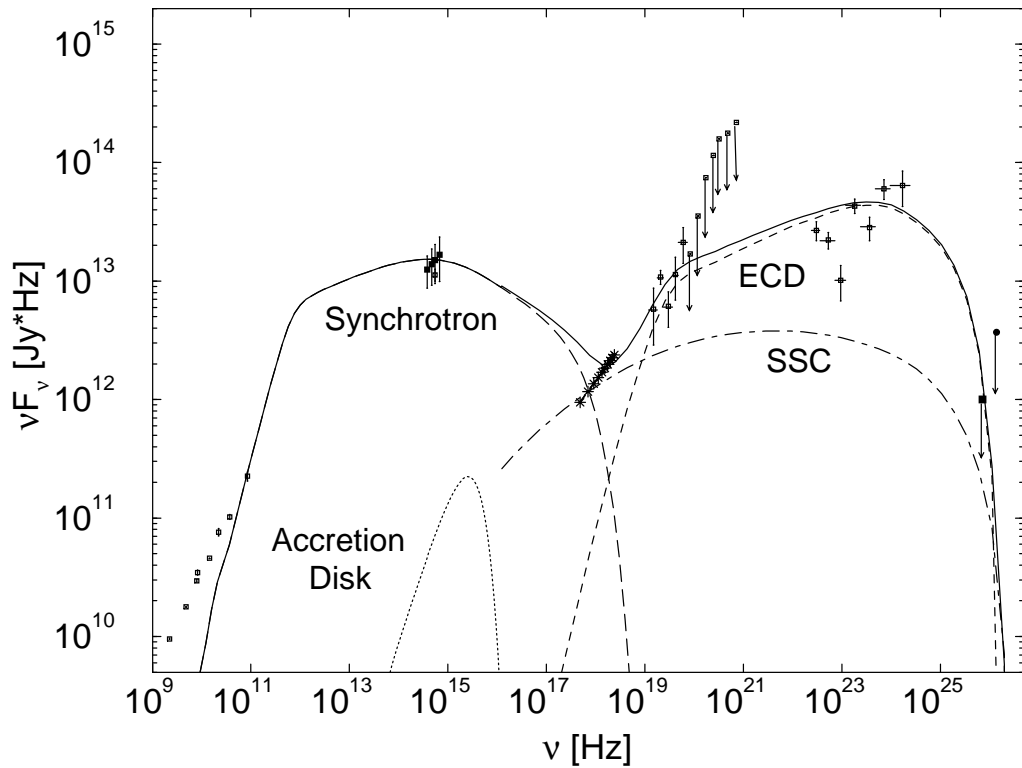


Fig. 2.— Attempt to fit the SED of BL Lac with an ECD-dominated model. Parameters: $\gamma_1 = 30$, $\gamma_2 = 10^5$, $s = 2.6$, $B' = 0.8$ G, $\Gamma = 20$, $\theta_{obs} = 2^\circ$, $n'_e = 400$ cm $^{-3}$, $R'_B = 2 \cdot 10^{16}$ cm, $z_i = 7 \cdot 10^{-3}$ pc, $M_6 = 100$, $f = 1$

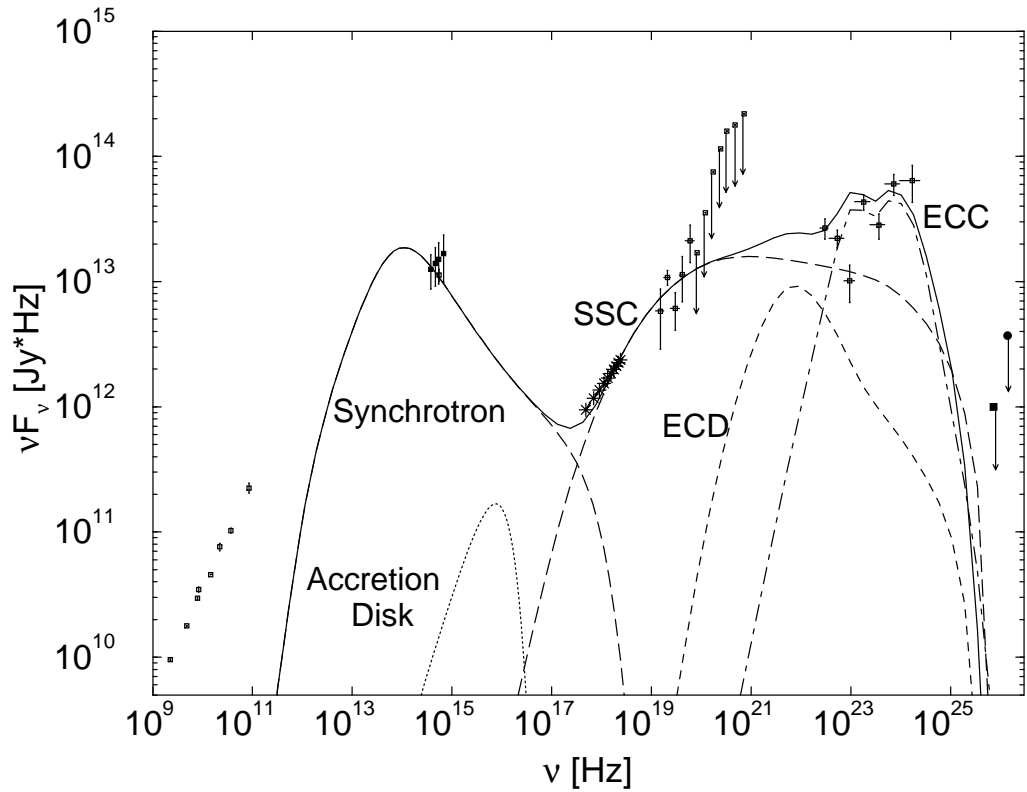


Fig. 3.— Fit to the SED of BL Lac with a combined SSC + ECC model. Parameters: $\gamma_1 = 500$, $\gamma_2 = 3.5 \cdot 10^4$, $s = 2.5$, $B' = 9$ G, $\Gamma = 15$, $\theta_{obs} = 3^\circ$, $n'_e = 3 \cdot 10^3$ cm $^{-3}$, $R'_B = 1.2 \cdot 10^{15}$ cm, $z_i = 5 \cdot 10^{-4}$ pc, $r_{in,BLR} = 5 \cdot 10^{-4}$ pc, $r_{out,BLR} = 6 \cdot 10^{-4}$ pc, $\tau_{T,BLR} = 0.025$, $M_6 = 2$, $f = 0.8$